Experimental Study of the Effects of Hypoxia Simulator on Osteointegration of Titanium Prosthesis in Osteoporotic Rats

Jiangfeng Liu
Third Hospital of Hebei Medical University
Huijun Kang
Third Hospital of Hebei Medical University
Jiangfeng Lu
Third Hospital of Hebei Medical University
Yike Dai
Third Hospital of Hebei Medical University
Fei Wang (wfljf2020@126.com)
Third Hospital of Hebei Medical University

Research Article

Keywords: Deferoxamine, Osseointegration, Osteoporosis, Arthroplasty, Titanium prosthesis

Posted Date: April 7th, 2021

DOI: https://doi.org/10.21203/rs.3.rs-379490/v1

Version of Record: A version of this preprint was published at BMC Musculoskeletal Disorders on November 11th, 2021. See the published version at https://doi.org/10.1186/s12891-021-04777-6.

Abstract

Purpose: Poor osseointegration is the key reason for implant failure after arthroplasty, whether in osteoporotic or normal bone conditions. To date, osseointegration remains a major challenge. Recent studies have shown that deferoxamine(DFO) can accelerate osteogenesis by activation of the hypoxia signal pathway. The purpose of this study is to test the following hypothesis: after knee replacement, intra-articular injection of DFO will promote osteogenesis and osseointegration with titanium prosthesis in the bones of osteoporotic rats.

Materials and Methods: 90 female sprague-dawley rats were used for the experiment. Ovariectomy and knee arthroplasty were performed. Then, the rats were randomly divided into DFO and control group(n=40 per group). The two groups were treated by intraarticular injection of DFO and saline respectively. After 2 weeks, polymerase chain reaction(PCR) and immunohistochemistry were used to evaluate the levels of HIF-1a, VEGF and CD31. After 12 weeks, the specimens were examined by micro CT, biomechanics and histopathology to evaluate osteogenesis and osseointegration.

Results: The results of PCR showed mRNA levels of VEGF and CD31 in DFO group were significantly higher than those in control group. The immunohistochemistry results indicated positive cell expressions of HIF-1a, VEGF and CD31 in DFO group were also higher. Compared to control group, the microCT parameters of BMD, BV/TV, TB.N, TB.Th were significantly higher. The maximal pull-out force and the bone-to-implant contact (BIC) value were also higher .

Conclusions: The local administration of DFO which is used to activate HIF-1a signaling pathway can promote osteogenesis and osseointegration with the prosthesis in osteoporotic bone.

Introduction

Implant stability and long-term success of total knee arthroplasty (TKA) depend on component fixation that can either be cemented or cementless[1][2]. Prosthesis stability not only depends on good initial mechanical stability, but also depends on late osseointegration, whether in normal or in osteoporotic bone. However, the majority of patients undergoing arthroplasty are older people who have varying degrees of osteoporosis. Osteoporosis is characterized by bone resorption exceeding bone formation, low bone mass, and microstructural degeneration[3]. Recent studies have indicated that low bone mass around prostheses leads to initial instability, aseptic loosening, periprosthetic fracture, and an increased rate of revisions. Moreover, relevant problems associated with low bone mass around prostheses in osteoporosis patients are more obvious [4][5][6][7]. Therefore, it is necessary to take measures to increase the amount of bone around the prosthesis and improve the rate of osseointegration to prevent prosthesis loosening. Additionly, biological enhancement of cancellous bone quantity and osseointegration will provide one mechanism to improve the outcomes of cementless total knee arthroplasty. Unfortunately, there is still no good solution for protecting bone mass around prostheses.Currently, in addition to better

prostheses and improved surgical techniques, many drugs are used to strengthen bone formation around the prosthesis and osseointegration in experiments [8][9][10][11][12].

Studies have shown bone regeneration can be promoted by activating hypoxia inducible factor-1a (HIF-1a) signal pathway through hypoxia-mimicking drugs or related genetic manipulation. HIF-1a, as a response element, can stimulate the production of vascular endothelial growth factor (VEGF) when combined with the target gene, and finally promote new bone formation through the angiogenic-osteogenic coupling pathway[13][14][15]. Deferoxamine (DFO) is an iron chelator, which has recently been widely studied as a hypoxia simulator. Ferric iron is a critical cofactor for prolyl hydroxylase (PHD) proteins involved in the oxygen dependent regulation of HIF-1a, and chelation results in the unrestricted activation of HIF-1a. Researches have shown that local administration of DFO can promote the formation of new bone which has been confirmed in fracture, distraction osteogenesis and bone defect animal models[16][17][18][19][20][21]. Even some experiments have shown that DFO can promote bone formation under abnormal bone conditions such as osteoporosis, pathological fracture caused by radiation[22][23][24]. Jia et al. [25] reported that DFO enhanced healing of osteoporotic bone defect via enhanced angiogenesis and osteogenesis. However, it is unclear whether DFO can promote the osseointegration of titanium prosthesis in osteoporotic bone after knee replacement.

Although the blood supply of cancellous bone is abundant in osteoporotic bone, the expression of HIF-1a and VEGF in osteoporotic bone is lower than that in normal bone, and H-type blood vessels decrease, then the ability of neovascularization declines and local osteogenesis gradually decreases[26]. The loss of bone mass ultimately leads to increased fracture incidence and prosthesis loosening rate after arthroplasty. So, it is possible to increase new bone mass by using drugs to promote neovascularization around implants after prosthesis implantation. In the current study, we will determine whether local administration of DFO to activate HIF-1a signaling pathway can augment the cancellous mass around implant and osteointegration by using our implant model in osteoporotic rats.

Materials And Methods

All the animals used were from the Experimental Animal Center of Hebei Medical University. All procedures involving animals are in compliance with the "Animal Care and Use" guidelines and approved by the Animal Care and Experimental Committee of the Third Affiliated Hospital of Hebei Medical University. ID of the ethics approval is Z2018-005-1.

Prosthesis design

The shape and size of the upper tibia, including the medullary cavity, were observed and measured on the transverse, coronal and sagittal planes by dissecting the upper tibia of the rats. Then, a tibial knee replacement (hemiarthroplasty) was designed to replace the tibial articular surface. Based on the implant shape showed in human knee replacement, a press-fit titanium tibial implant comprised of an articular baseplate and intramedullary stem. The baseplate surface was oval in shape with a medial–lateral width

of 7.0mm anterior–posterior depth of 5.0mm and thickness of 1.5mm. The area of the baseplate was similar to that of the tibial plateau of rat, which formed joint with femoral condyle. The stem was approximately columnar with 5.0mm in length and 1.5mm in diameter . So as to make the prosthesis stable, one side of the stem was attached a small wing, which could not only prevent the prosthesis from rotating in the bone, but also better adapt to the shape of the medullary cavity of the upper tibia of rats. The 3D image of prosthesis was simulated by computer-aided design, and then the prosthesis was made by 3D powder printer (Arcam Q10, Sweden) with titanium powder. The powder was spherical in shape with a median size of approximately 40 μm (Fig. 1). The articular surface was polished using 1,200 grit silicon carbide grinding paper, and the stem surface was coated with close-packed 40-μm-diameter titanium spheres which made the surface rough and beneficial to bone ongrowth. Implants were degreased and cleaned by using Alconox detergent (Seebio, Xi'an, China) and sonication in deionized water. Before implantation, the grafts were sterilized by using a standard autoclave (121℃; humidity 100%; 30min).

Establishment of osteoporosis rat model

90 two-month-old female Sprague Dawley (SD) rats were obtained from Laboratory Animal Center of Hebei Medical University (Shijiazhuang, China) and housed in the Research Animal Facility. The facility is controlled by temperature, ventilation, and illumination. Rats were fed standard hard chow and water ad libitum. When the rats reached three months old, five rats were randomly designated as members of the sham group. The remaining rats were subjected to ovariectomies (OVX) to simulate osteoporosis models. Preoperative subcutaneous injections of gentamicin (5mg/kg) were administered to protect from infection. Anesthesia was successfully achieved by intraperitoneal injection of 1.5% phenobarbital sodium 40mg/kg (Schering-Plough, Belgium). One small incision (1.5cm) was made through the skin and the muscle wall on each side of the backbone in the dorsal aspect, and the bilateral ovaries were exposed and removed from OVX animals. In the sham animals, only a small amount of fat around the ovaries was removed. The wound was sutured in layers. After 3 months, five sham rats and five OVX rats were sacrificed, and the BMD of the fifth lumbar of each rat was measured by using dual-energy X-ray absorptiometry (DEXA; Lunar Corporation, USA). A reduction in bone mineral density of more than 20% was considered as a successful model of osteoporosis[27][28].

Prosthesis implantation surgery

After identifying osteoporosis in rats, a unilateral (left) tibial knee replacement was performed on each animal. The skin over the left knee was sterilized twice with alcohol. The fur was removed with a hair razor. Preoperative subcutaneous injections of gentamicin (5mg/kg), buprenorphine (0.03mg/kg) were administered. After successful anesthesia according to the methods mentioned above, the operation area was covered with sterile sheet leaving only the knee joint exposed. The knee was opened with a parapatellar medial incision and the tendon with the patella was dislocated laterally. After the joint cavity was exposed completely, the anterior cruciate ligament and menisci were resected, and the posterior cruciate ligament was reserved. Bone scissors were used to remove articular cartilage and proximal

epiphysis to accommodate the implant. The thickness of the cut bone is about 1.5mm, which is equivalent to the prosthesis tray.A hand drill was used to drill a 1-mm wide and 5-mm deep hole in the tibia to fit the stem of the prosthesis. After washing bone surface with aseptic water, the prosthesis was implanted in a press-fit manner (cementless). Ethibond 4-0 suture was used to close the joint capsule and Vicryl 5-0 suture was used to close the skin (Fig. 2). After the operation, the knee joint is stable and can be extended and flexed as normal.

Delivery of DFO

Subsequently, the rats were randomly divided into DFO group (n = 40) and control group (n = 40). Starting on postoperative day 4, all rats in DFO group were injected with 200uL of 200umol DFO solution (Sigma, St. Louis, MO, USA) in normal saline directly into the knee joint cavities. The rats were mildly sedated before injection, and a 25-gauge needle was used to deliver the solution carefully (Fig. 2). The rats in control group were injected with 200uL of normal saline in an identical manner. The procedure was repeated every 48h for a total of six doses. The DFO dose and injection schedule were based on previous review of the literature[16][18][20].

Postoperative course

After the operation, rats were allowed free motion and unrestricted access to food and water. All rats were monitored daily for signs of inflammation, lethargy, and for general health by an experienced animal care technician. Two hours after the surgery, injections of buprenorphine at 0.01mg/kg (Schering-Plough, Belgium) were administrated and continued at 0.005 mg/kg for three days. After that, an X-ray examination was performed to confirm that the implant was in a satisfactory predetermined position. We found no knee dislocation or subluxation, which proved that the joint was stable. We also found there was no periprosthetic gap visible to the naked eye on radiographs, which meant the prosthesis and bone were in close contact (Fig. 2).

After 2 weeks of implantation, euthanasia was performed by overdosing 8 rats of each group with sodium thiopental at 90 mg/kg (Schering-Plough, Belgium) after an overdose of anesthaesia. Proximal tibia was explanted, the bones were stripped of surrounding soft tissue and the prosthesis was removed, then the bones were fixed in cold 4% formaldehyde for 1 day for immunohistochemical examination. Another 16 rats (8 rats in each group) were euthanized in the same way. The bone tissue was cut into about 0.5× 0.5 ×0.5 cm in size. The whole process was completed within 30 minutes. Afterwards the samples were put into the sterile cryopreservation tube, pre-cooled in liquid nitrogen for 5 minutes, and finally stored in liquid nitrogen tank(-80℃) for PCR. Three months after knee surgery, all rats from each group were sacrificed in the same way. All tibias containing the stabilized prosthesis were stripped of surrounding soft tissue, and subjected to micro-CT analysis, histopathology and biomechanical testing as detailed below.

Quantitative real-time reverse transcription PCR

The expressions of vascular endothelial growth factor (VEGF) and vascular endothelial cell marker CD31 were detected by RT-PCR. Total RNA was extracted by the TRIZOL protocol (Sigma-Aldrich, MO), then was concentrated and purified according to the instructions. RNA integrity was measured by using agarose gel electrophoresis (AGE). A Prime-Script First-Strand cDNA Synthesis Kit (Takara, Dalian, China) was used for reverse transcription. An SYBR® premix Ex TaqTM kit (Takara, Dalian, China) was used for PCR amplification. Real-time quantitative PCR was performed at 57°C for 30 cycles in the Opticon Continuous Fluorescent Detector by using IQTM SYBR green supermix (BioRad, USA). Each group of samples was repeatedly measured three times. $2^{-\triangle\triangle CT}$ was used to analyze the relative expression of each group of genes.Rat 18S ribosomal RNA was used as internal reference. The following primers were used (Table 1).

Table 1. Primers for Real-Time PCR Analysis

Gene	Forward Premier	Reverse Premier
VEGF	AGAAAGCCCATGAAGTGGTGA	GCTGGCTTTGGTGAGGTTTG
CD31	TTGTGACCAGTCTCCGAAGC	TGGCTGTTGGTTTCCACACT
Rat-18sRNA	GTAACCCGTTGAACCCCATT	CCATCCAATCGGTAGTAGCG

Immunohistochemistry

At the same time, immunohistochemistry was also performed to assess the expression of HIF-1a,VEGF, CD31, as well as to assess the angiogenic potential of periprosthetic bone tissue. Briefly, the upper tibial bone tissue from which the prosthesis was removed was fixed, decalcified, embedded in paraffin, and sliced to a thickness of 5mm. The sections were deparaffinized and washed with PBS. The slice was immersed in 3% hydrogen peroxide for 10min to block endogenous peroxidase activity and then were rinsed several times in PBS. After being blocked with 1% BSA solution at room temperature for 1 hour, sections were treated with a primary antibody overnight at 4℃ and incubated with the biotinylated secondary antibody for 30min. Negative control sections were incubated with PBS solution. The following specific antibodies were used: HIF-1a, HIF-2a (Upstate Biotechnology, Lake Placid, New York, USA), VEGF (Upstate Biotechnology, Lake Placid, New York, USA), CD31 (Santa Cruz biotechnology, Dallas, Texas, USA). Next, the slides were visualized using a streptavidin-biotin staining technique that involves peroxidase labeling. The nuclei were counterstained with hematoxylin. The sections were observed by optical microscope (Olympus BH-2, Japan) and photographed by the high performance computer-aided image analysis system (Nikon H600l, Japan). The yellowcolored cells were considered antigen-positive. Then, the image analysis software (Image Pro Plus 6.0 software) was used for quantitative analysis of the positive staining images.Ten randomly fields in bone marrowcavities in each section were selected to quantify the positive staining with the accumulated optical density value. The

ratio of the accumulated optical density value to the corresponding observation area was used as the final quantitative parameter and recorded as the mean optical density value (MOD). Eight sections for each protein from each group were analyzed. After immuohistochemical staining for CD31, the formation of microvessel could be observed by light microscopy. The observer was blind regarding the identity of two groups.

Micro-CT scan analysis

8 tibias were harvested and the attached soft tissues were excluded, and then the gross specimens were observed. After the prosthesis was removed gently, the bone around the prosthesis was examined by high-resolution micro CT (skyscan1176; skyscan, knotich, Belgium). The setting parameters of μCT were as follows: resolution ratio, 45 mm; volume, 50 kV; current, 500 UA. 2mm thick bone around the prosthesis was used as the volume of interest (VOI) (Fig.3). The change in the amount of cancellous bone depends not only on the distance from the joint surface, but also on the distance from the cartilage growth zone. The implantation was a standardized operation. When we implanted the prosthesis, the stem passed through the growth plate. The distal end of the prosthesis was 6.5mm under the joint surface and 4.5mm under the growth plate. Continuous scanning was performed from the proximal to distal tibia along the longitudinal axis of the tibia. The scanning length was 5 mm and the layer thickness was 18 um. Then 3D reconstruction of the trabecular bone was performed, bone mineral density (BMD), ratio of bone volume to tissue volume (BV/TV), trabecular thickness (Tb.Th), trabecular separation (Tb.Sp), and trabecular number (Tb.N) of the VOI were calculated by Mimics 19.0 software (Materialise, Leuven, Belgium).

Biomechanics

WWD-10A electronic universal testing machine controlled by microcomputer (Sanfeng Instrument Technology Co., Ltd. Changzhou, China) was used to pull out the prosthesis of two groups of samples. Following euthanasia, 8 tibias were harvested and surrounding soft tissue was removed carefully. The proximal bone and prosthesis were exposed clearly. Two ends of tibia specimen and prosthesis were fixed with self-curing plastic(Methyl methacrylate) respectively. Two 1mm diameter steel wire ropes were respectively reserved in the self-curing plastic at both ends. The steel wire ropes were connected with the clamps at both ends of electronic universal testing machine to keep the longitudinal axis of tibia perpendicular to the horizontal line of the ground. The axial and lateral stress of the prosthesis must be avoided during the whole mechanical process. The load measurement accuracy of the tester is 0.01N, and the loading speed is 0.1mm/s. Pull-out test is carried out to check the intensity of osseointegration. The stress-time curve is described by the self-contained software, and its peak value is the maximum pull-out force.

Histopathology

Following euthanasia, 8 retrieved upper tibial bone including implants were processed for undecalcified histology. After fixation in 4% paraformaldehyde for 48h, the implants were rinsed in water for 24h, dehydrated in ethanol step by step, cleared in xylene for 12h, and embedded in polymethyl methacrylate resin (Leica Microsystems GmbH, Wetzlar, Germany). After sufficient polymerization, each implant was cut along its vertical axis giving 7-8 sections by using hard tissue slicer (SP1600 Leica Microsystems Concord, ON, Canada). The location of the histological section was 1.5mm from the distal end of the prosthesis. The thickness of each slice was 70um, and three most central sections from each specimen were kept for polishing, staining with 1% toluidine blue and histological analysis. Semi-automatic digital image analysis system of bone morphology was used for histomorphometric analysis. The system includes microscope (Olympus BX51, Japan), digital camera (Nikon H600L, Japan) connected with computer, and bone morphometry analysis software (Bioquant, USA). Bone-to-implant contact (BIC) value is the ratio of the length of direct contact between the surrounding bone tissue and the implant body to the total circumference of the implant body. BIC value can be calculated by software to indicate the degree of bone integration.

Statistical analysis

Before the investigation, the sample size was estimated by using bone-implant contact (BIC) as the primary variable. On the basis of our pilot studies , the standard deviation was assumed at 13% in both experiment and control groups, and an estimated difference of 20% was determined between the groups. A power calculation was performed with a confidence level of 95% (α=0.05) and power (1-β) of 80%. This yielded an estimated sample size of 7 knees per group. We would use N=8 for every examination at each time point to account for potential unexpected losses of animals during our experiments.

All the data were described as mean±standard deviation. Student's t-test was used for comparison of means between the two groups (SPSS version 20.0), $p<0.05$ was determined to be significant.

Results

Confirming the rat osteoporotic model

Quantitative analysis by dual-energy X-ray absorptiometry showed that the BMD of lumbar trabecular bone in OVX rats was 0.263±0.021mg/cm^2, decreased by 23.35%, which was significantly lower than that of sham rats (0.343±0.022mg/cm^2; $p<0.05$; Fig. 4).

Effect of DFO on angiogenesis

Two weeks after the implantation, the mRNA levels of VEGF and CD31 were detected by real-time quantitative PCR. DFO significantly upregulated the mRNA expression levels of VEGF which is a very important angiogenic factor in the HIF-1a pathway [$P<0.05$, Fig. 5(A)]. The increase of mRNA of CD31 showed more significant angiogenesis in DFO group [$P<0.05$, Fig. 5(B)]. The results of immunohistochemistry showed that the positive granules of HIF-1a and VEGF in the sections of DFO

group were significantly more than those in control group[Fig. 6(A)], and the mean optical density value was significantly higher compared with the control group[P<0.05, Fig. 6(B)]. We used endothelial cell marker CD31 to monitor the formation of vascular network, and found that more CD31 positive cells formed tubular structure in DFO group than in control group[P<0.05, Fig. 6(A)]. The expression levels of HIF-2a in both groups were also examined. However, There was no significant difference in the number of positive granulosa cells between the two groups, The mean optical density of DFO group was slightly higher than that of control group, but the difference was not statistically significant[P>0.05, Fig. 6(B)].

Effect of DFO on bone formation and integration

After 12 weeks of implantation, it could be seen that the osseointegration of the prosthesis was good without loosening or displacement in gross specimens [Fig. 2 (H-I)]. We considered that the good osseointegration detected by naked eye had no displacement such as sinking, tilting and rotation, meanwhile the prosthesis could not be removed by forceps clamping. But in the control group, there was a small cyst in the tibial plateau in 2 cases after pulling out the prosthesis. After implantation, we had X-ray examination of the rat knee joint, and found no prosthesis loosening or displacement.

After the prosthesis was withdrew, microCT was used to evaluate new bone formation around the prosthesis. The morphology of new bone were quantitatively analyzed by microCT images, 3D reconstruction and microstructure parameters. The result of microCT showed that more bone tissue formed around the prosthesis in DFO group, and the density and magnitude of bone trabeculae in DFO group were higher than those in control group. In control group, the bone structure was sparse and loose, and the trabecular structure was disordered, which was not consistent with the direction of main trabecula. BV/TV, TB.N, TB.Th and BMD for DFO group were significantly higher than they were for control group, while TB. SP for DFO group was significantly lower than it was for control group [$P < 0.05$, $P < 0.05$, $P < 0.05$, $P < 0.05$, $P < 0.05$, respectively; Fig. 7 (A-F)].

The biomechanical bond strength of bone-implant interface was measured by pull-out test. The result showed that the maximum pullout force (118.7 ± 14.4N) for DFO group was significantly higher than it was for control group (97.1 ± 15.2N), and the difference was statistically significant ($P < 0.05$; Fig. 8).

It can be seen from the undecalcified histological sections that more bone tissue in DFO group combined with the implants directly. MIC in DFO group (60.6±5.4%) was significantly higher than that in control group (44.9±3.3%), and the difference was statistically significant ($P < 0.05$; Fig. 9). In DFO group, a small amount of soft tissue membrane surrounded the prosthesis, while more soft tissue membrane was found in the control group.

Discussion

In this study, we designed knee prosthesis for rats and created a novel animal model of knee replacement. By implanting the prosthesis into the osteoporotic proximal tibia, it was found that local administration of the hypoxia simulant deferoxamine to activate HIF-1a signal pathway could increase

the osteogenesis around the prosthesis in osteoporotic bone, promote the osseointegration, and improve the stability of the prosthesis. The results from microCT showed BV/TV, TB.N, TB.Th and BMD of bone trabeculae around the prosthesis were significantly increased, and Tb.Sp decreased obviously, which meant the degree of osteoporosis improved. Biomechanical experiment results demonstrated that the binding force between the prosthesis and the surrounding bone increased significantly. Results obtained from histopathological analysis showed bone-implant integration also increased.

In the experiment, we successfully made the animal model of knee replacement in osteoporotic rats through two sequential operations. In the first operation, traditional ovariectomy was used to model osteoporosis, which is a traditional and successful method. It can well simulate the osteoporosis model of elderly patients because of estrogen deficiency in postmenopausal women[28]. First of all, we used the animal model of osteoporosis in order to be more close to the bone characteristics of the elderly patients undergoing joint replacement. In the second operation, tibial articular surface of the knee joint was replaced by cementless fixation to make the animal model of hemiarthroplasty of knee, which was different from prior animal model, because most of the models of bone integration were established by implanting titanium rod or screw outside or inside the joint[29][30][31][32][33]. Niels et al. [34]used alloy prosthesis on the femur side and high density polyethylene prosthesis on the tibia side, both with cementless fixation to made knee replacement model, but the prosthesis was loose and displaced after the operation. Kenneth[35] used polyetheretherketones(PEEK) material to make a rat model of tibial knee replacement, which was fixed with bone cement successfully. Carli[36] et al. made a mouse model of tibial knee replacement with titanium prosthesis. It is an innovation that we used titanium prosthesis to make a knee replacement model in rats. Of course, the knee joint in humans and rats are very different. The human knee bears weight in extension, while the rat knee bears weight in flexion. In addition, there are differences in the range of motion and the angle of motion for knee joint when walking. However, the main functions of the knee in rats are weight-bearing, stretching and flexing. Our prosthesis can meet these functions. However, due to the lack of a stable device on the sagittal plane, we are worried about the risk of forward dislocation of the knee joint. It is gratifying that we did not find the occurrence of joint dislocation in the postoperative physical and X-ray examination.The theory of human joint stability may not apply to rats. The rats used the operatively treated leg normally througtout the postoperative period with no gait alterations after the immediate postoperative period. This observation suggests that the rats were bearing weight. What is different from previous studies in the non-weight-bearing state is that we are studying the osseointegration of animals in the weight-bearing state , which is closer to the clinical practice. It is the first time for us to use this kind of physiologically loaded intra-articular rat model, but we used a similar implant in tibia of mice before. This model is a viable platform on which to study pharmacologic enhancement of the bone-implant interface.

The dosage used in this experiment is recommended by referring to the previous literature[37][38]. This dose can produce obvious effect in many experiments, including distraction osteogenesis, fracture healing, and promoting osteointegration of artificial bone in repairing segment defect of long bone, and no serious side effects have been reported. Therefore, we also adopt this dose in our study. Further

research is needed to determine the optimal dose. The time period of administration is just the active period of tissue repair, which can make the drug play an active role in the largest. We adopted the method of intra-articular injection for local administration, which could make the drug penetrate around the prosthesis and bone and play a pharmacological function. Due to the narrow joint cavity of rats, only a small amount of saline (200ul) was used for drug dissolution to prevent excessive drug extravasation. We chose 2 weeks and 3 months after operation as observation time points. 2 weeks after operation is the time when blood vessels and scar tissue form vigorously, which is conducive to the detection of cytokines. Three months after surgery, the drug effect may disappear, but mature bone has formed. We paid more attention to the mature and stable bone tissue around the prosthesis, which could maintain the long-term stability of the implant.

Deferoxamine is a hypoxia simulator. It can inhibit activity of prolyl hydroxyprolidase (PDH) by combining with iron, thus causing the accumulation of HIF-1a in the nucleus. Through combining with the target gene, HIF-1a can stimulate the production of VEGF and promote the regeneration of blood vessels. Blood vessels not only transport necessary oxygen and nutrition for the regeneration of bone, but also transport growth factors and bone progenitor cells which is also necessary for bone formation. Through regulating the interaction among osteoblasts, osteoclasts, bone cells and vascular cells, local bone growth is promoted[16][21][39][40][41][42]. Lowered levels of angiogenic factors, such as vascular endothelial growth factor(VEGF), and the resulting reduction in the rate of bone vessel formation, are causes of poor bone repair. Therefore, the basic strategies for enhancing osteoporotic bone regeneration are to promote osteogenesis or angiogenesis. We can also use drugs to inhibit bone resorption, such as bisphosphonates[43]. Hypoxia is one of the main driving forces of angiogenesis-osteogenesis coupling. HIF is the key regulator of the coupling mechanism. Farberg et al. [23] reported in the study of distraction osteogenesis that DFO injection into the distraction gap of bone can enhance the activity of all cells, including bone precursor cells and endothelial cells. As long as DFO solution reaches the site, new bone formation can be obviously seen [44]. Studies have shown that local administration of DFO into fracture sites can promote fracture healing in long bone[16][17]. Drager et al. [20] implanted microporous dicalcium phosphate dihydrodrate (brushite) grafts in the bone defects of rabbits and found that local injection of DFO could significantly promote bone integration. After topical administration of DFO carried by polylactic acid scaffold to osteoporotic bone defect in rat experiment, Jia et al. [25] found that vascular networks appeared denser around the DFO-containing scaffolds than they did around the untreated scaffolds, which finally promoted the new bone formation and repair of bone defect. In this study, it is found that local administration of DFO can promote the regeneration of blood vessels and bone around the implant in osteoporotic bone, and ultimately promote the osseointegration.

PCR results showed that the mRNA levels of VEGF and CD31 were higher in DFO group than those in control group, which demonstrated abundant angiogenesis was involved in this osteogenesis process. This result was also confirmed in immunohistochemistry. We adopted immunohistochemical method to detect the expression of HIF-1a and HIF-2a in the two groups, because DFO could also stabilize HIF-2a protein and further up-regulate the expression of VEGF. The results showed there was only a small

amount of HIF-2a expression in the two groups, and there was no difference between the two groups, but more HIF-1a protein was found in DFO group, proving that DFO acts by stabilizing the expression of HIF-1a. So, in our study the bone formation around the prosthesis is promoted through HIF-1a/VEGF pathway, at least partially. Hypoxia is a powerful stimulus to angiogenesis. VEGF is the most powerful angiogenic factor in the downstream of HIF-1a pathway[13]. It can promote the proliferation, migration and tubular formation of endothelial cells by binding with specific receptors of vascular endothelial cells. In the immunohistochemistry experiment, the positive rate of CD31 in the experimental group significantly increased, and there were many clusters of positive cells, which proved the existence of a large number of neovascularization, while the expression level of CD31 in the control group was very low. Rena et al. [45] used biodegradable calcium phosphate complex to fill the defect in the rat model of femoral defect. After DFO was given locally, the effect of angiogenesis was obviously enhanced. The number of blood vessels examined by angiography in the DFO group was twice as much as that in control group.

After implantation, we made X-ray examination of the rat knee joint, and found no prosthesis loosening or displacement. We also found no loosening in the gross specimen. From the results of microCT, it could be seen that compared with the control group, BMD, BV/TV, TB.N, TB.Th in DFO group increased significantly, while TB. SP decreased, which indicated that the bone formation around the prosthesis increased, and the degree of osteoporosis improved. Jia et al. [25] implanted polylactic acid scaffold with DFO to the bone defect of femur in osteoporosis rats. One month after operation, results from micro-CT data showed that more bone regenerated in DFO implantation group，BV/TV, Tb.N, and Tb.Th for the DFO group were significantly higher than they were for control group, which was consistent with the results of this study. From this study, it is believed that the enhancement of bone formation around the prosthesis will inevitably increase bone integration, thus enhancing the long-term stability of the prosthesis. Zhou et al. [10] performed the implantation of prosthesis in knee of rats and concluded that the stability of the prosthesis was enhanced after the bone mass and bone density around the prosthesis were increased, which is consistent with our view. It is important to observe the stability and the gap between the bone and the implant, but it is very difficult to detect the size of the gap using micro CT because of the artifacts produced by the metallic implant. Therefore, we pulled out the prosthesis and detected the bone mass around the prosthesis to infer the osseointegration indirectly. More bone mass around the prosthesis means better osseointegration. Implant removal has an effect on Micro CT and immunohistochemistry. When removing the implants, a small amount of bone tissue will be taken away due to osseointegration, which will reduce the bone mass around the prosthesis. The irregular contour of the inner bone surface due to the loss of bone mass can be seen on CT images. Therefore, we pulled out the prosthesis very gently to prevent excessive bone loss.

The biomechanical results showed that the maximum pull-out force for DFO group was significantly higher than it was for control group, indicating that DFO can promote the strength of osseointegration of the prosthesis and improve the stability of the prosthesis. The degree of bone integration can be seen more directly from the results of histopathological sections. Drager et al. [47] found that local administration of DFO can promote the integration of artificial bone graft and host bone through animal

experiments. Yu et al. [48] implanted the titanium prosthesis adhered by DFO into the bone of rats, and observed that the bone growth around the prosthesis was significantly enhanced. Although there are no cases of implant loosening, we think that if the observation time is prolonged, it will be possible to find cases of implant loosening.

Our results show that using DFO to activate HIF-1a signal pathway can increase angiogenesis and further promote bone growth and integration with the implant. The mechanisms by which bone growth is promoted are complex. DFO can inhibit the differentiation and function of osteoclast through RANKL/OPG pathway, thus reduce the loss of bone mass. In addition, DFO can also enhance the classic Wnt/ß-catenin signaling pathway in Osteoblasts, promote BMSCS to osteoblast differentiation and strengthen osteoblast activity, and ultimately promote bone formation[46] [48]. Moreover, HIF-1a not only up-regulates VEGF to promote vasculogenic-osteogenic pathway, but also directly regulates osteoblasts and promotes the proliferation, differentiation and mineralization of osteoblasts. HIF-1a also enhances the Wnt/ß-catenin signaling pathway and regulates the expression of target gene Runx2, which promotes mesenchymal stem cells differentiation into osteoblasts, with the involvement of a variety of cytokines. This is a relatively independent mechanism of VEGF [49][50]. HIF-2a can also regulate angiogenesis and bone growth, but it mainly plays a role in chronic hypoxia[51]. Further exploration of these mechanisms can lead to a better understanding and help to propose new treatment for promoting osteointegration.

The idea that osteoporotic patients can be treated with TKA has been widely accepted. More attention has been focused on how to improve the success rate. Long-term success of orthopedic implants is largely dependent on the degree of osseointegration with the surrounding bone. The trabecular bone of osteoporotic bone is sparse and thin, and the mechanical support force to prosthesis is insufficient compared with normal bone, which can lead to cancellous bone bearing the construct collapse, resulting in prosthesis displacement and subsidence, and can also cause periprosthetic fracture. Therefore, increasing the bone mass around the prosthesis is a very important preventive measure.

This study suggests that the local administration of DFO to activate HIF-1a signaling pathway can promote osteogenesis and osseointegration with the prosthesis in osteoporotic bone. DFO can provide a potential therapeutic target and treatment scheme for osteoporotic bone integration. In this study, no complications such as infection and necrosis were found in rats after administration of DFO.In addition, DFO is cheap and widely used, which means that DFO has an encouraging prospect. Although the knee replacement model is used in this study, we speculate that the experimental results are also instructive for hip replacement. There are two points to be improved in the future. First, try to design the tibial prosthesis into the shape similar to meniscus with high perimeter, which is more conducive to the stability of the joint. Second, whether systemic administration of DFO can promote bone integration is a subject worthy of research, after all, there are studies that have shown systemic administration could improve osteoporosis.

Declarations

Statement:

The study was carried out in compliance with the ARRIVE guidelines.

Ethics approval and consent to participate: The study was approved by the Animal Care and Experimental Committee of the Third Affiliated Hospital of Hebei Medical University.

Consent for publication: All the authors agreed to publish this paper.

Availability of data and materials: All data generated or analysed during this study are included in this published article.

Competing interests: No potential conflict of interest was reported by the authors.

Funding: The study was financially supported by the National Natural Science Foundation of China (No. 81371910).

Authors' contributions: Wang Fei designed the experiment protocol. Liu Jiangfeng and Lu Jiangfeng conducted the experiment. Liu Jiangfeng wrote the main manuscript text. Dai Yike and Kang Huijun prepared figures1. Liu Jiangfeng and Lu Jiangfeng prepared figures2. Liu Jiangfeng prepared figuare3-9. All authors reviewed the manuscript.

Acknowledgments: The authors thank all colleagues in the central laboratory of the third hospital of Hebei medical university.

References

1. Dalury DF. Cementless total knee arthroplasty: current concepts review. Bone Joint J. 2016; 98-B(7):867-873. doi:10.1302/0301-620X.98B7.37367.
2. Vertullo CJ, Graves SE, Peng Y. Lewis PL. The effect of surgeon's preference for hybrid or cemented fixation on the long-term survivorship of total knee replacement. Acta Orthop. 2018; 89(3):329-335. doi:10.1080/17453674.2018.1449466.
3. Kanis JA, McCloskey EV, Johansson H, Oden A, Melton LJ, Khaltaev N. A reference standard for the description of osteoporosis. Bone 2008;42(3):467-475. doi:10.1016/j.bone.2007.11.001.
4. Fini M, Carpi A, Borsari V, Tschon M, Nicolini A, Sartori M, Mechanick J, Giardino R. Bone remodeling, humoral networks and smart biomaterial technology for osteoporosis. Front Biosci (Schol Ed) 2010; 2: 468–482. doi:10.2741/s79.
5. Fini M, Giavaresi G, Torricelli P, Borsari V, Giardino R, Nicolini A, Carpi A. Osteoporosis and biomaterial osteointegration. Biomed Pharmacother. 2004; 58(9): 487–493. doi:10.1016/j.biopha.2004.08.016.
6. Sartori M, Giavaresi G, Parrilli A, Ferrari A, Aldini NN, Morra M, Cassinelli C, Bollati D, Fini M. Collagen type I coating stimulates bone regeneration and osteointegration of titanium implants in the osteopenic rat. Int Orthopaedics. 2015; 39(10): 2041–2052.doi:10.1007/s00264-015-2926-0.

7. Aro HT, Alm JJ, Moritz N, Mäkinen TJ, Lankinen P. Low BMD affects initial stability and delays stem osseointegration in cementless total hip arthroplasty in women: a 2-year RSA study of 39 patients. Acta Orthopaedica. 2012;83(2):107–114. doi:10.3109/17453674.2012.678798.
8. Bondarenko S, Dedukh N, Filipenko V, Akonjom M, Badnaoui AA, Schwarzkopf R. Comparative analysis of osseointegration in various types of acetabular implant materials. Hip Int; 2018, 28(6): 622-628. Doi:10.1177/1120700018759314.
9. McClung M, Harris ST, Miller PD, Bauer DC, Davison KS, Dian L, Hanley DA, Kendler DL, Yuen CK, Lewiecki EM. Bisphosphonate therapy for osteoporosis: benefits, risks, and drug holiday. The American Journal of Medicine. 2013;126(1):13–20. Doi: 10.1016/j.amjmed.2012.06.023.
10. Zhou W, Liu Y, Shen J, Yu B, Bai J, Lin J, Guo X, Sun H, Chen Z, Yang H, Xu Y, Geng D. Melatonin increases bone mass around the prostheses of OVX rats by ameliorating mitochondrial oxidative stress via the SIRT3/SOD2 signaling pathway. Oxid Med Cell Longev, 2019(undefined), 4019619. doi:10.1155/2019/4019619.
11. Knusten AR, Ebramzadeh E, Longjohn DB, Sangiorgio SN. Systematic analysis of bisphosphonate intervention on periprosthetic BMD as a function of stem design. The Journal of Arthroplasty. 2014;29(6):1292-1297. doi:10.1016/j.arth.2014.01.015.
12. Guillot R, Pignot-Paintrand I, Lavaud J, Decambron A, Bourgeois E, Josserand V, Logeart-Avramoglou D, Viguier E, Picart C. Assessment of a polyelectrolyte multilayer film coating loaded with BMP-2 on titanium and PEEK implants in the rabbit femoral condyle. Acta Biomater. 2016;36: 310-22. doi:10.1016/j.actbio.2016.03.010.
13. Zou D, He J, Zhang K, Dai J, Zhang W, Wang S, Zhou J, Huang Y, Zhang Z, Jiang X. The bone-forming effects of HIF-1α-transduced BMSCs promote osseointegration with dental implant in canine mandible. PLoS ONE, 2012; 7(3): e32355. doi:10.1371/journal.pone.0032355.
14. Drager J, Harvey EJ, Barralet J. Hypoxia signalling manipulation for bone regeneration. Exp Rev Mol Med. 2015;17:e6. doi:10.1017/erm.2015.4
15. Maes C, Carmeliet G, Schipani E. Hypoxia-driven pathways in bone development, regeneration and disease. Nat Rev Rheumatol. 2012;8(6):358-366. doi:10.1038/nrrheum.2012.36.
16. Shen X, Wan C, Ramaswamy G, Mavalli M, Wang Y, Duvall CL, Deng LF, Guldberg RE, Eberhart A, Clemens TL, Gilbert SR. Prolyl hydroxylase inhibitors increase neoangiogenesis and callus formation following femur fracture in mice. J Orthop Res. 2009;27(10):1298-1305. doi:10.1002/jor.20886.
17. Donneys A, Ahsan S, Perosky JE, Deshpande SS, Tchanque-Fossuo CN, Levi B, Kozloff KM, Buchman SR. Deferoxamine restores callus size, mineralization, and mechanical strength in fracture healing after radiotherapy. Plast Reconstr Surg. 2013;131(5):711e-9e. doi:10.1097/PRS.0b013e3182865c57.
18. Donneys A, Farberg AS, Tchanque-Fossuo CN, Deshpande SS, Buchman SR. Deferoxamine enhances the vascular response of bone regeneration in mandibular distraction osteogenesis. Plast Reconstr Surg. 2012;129(4):850-856. doi:10.1097/PRS.0b013e31824422f2.
19. Zhang Weibin, Li Guosong, Deng Ruoxian, Deng Lianfu, Qiu Shijing. New bone formation in a true bone ceramic scaffold loaded with desferrioxamine in the treatment of segmental bone defect: a

preliminary study. J Orthop Sci. 2012; 17: 289-98. doi: 10.1007/s00776-012-0206-z.

20. Drager J, Ramirez-GarciaLuna JL, Kumar A, Gbureck U, Harvey EJ, Barralet JE. Hypoxia biomimicry to enhance monetite bone defect repair. Tissue Eng Part A. 2017; 23: 1372-1381.doi: 10.1089/ten.TEA.2016.0526.
21. 21.Wan C, Gilbert SR, Wang Y, Cao X, Shen X, Ramaswamy G, Jacobsen KA, Alaql ZS, Eberhardt AW, Gerstenfeld LC, Einhorn TA, Deng L, Clemens TL. Activation of the hypoxia-inducible factor-1alpha pathway accelerates bone regeneration. Proc. Natl. Acad. Sci. U.S.A. 2008;105(2): 686-91. doi:10.1073/pnas.0708474105.
22. Donneys A, Weiss DM, Deshpande SS, Ahsan S, Tchanque-Fossuo CN, Sarhaddi D, Levi B, Goldstein SA, Buchman SR. Localized deferoxamine injection augments vascularity and improves bony union in pathologic fracture healing after radiotherapy. Bone. 2013; 52(1): 318-25. doi:10.1016/j.bone.2012.10.014.
23. Farberg AS, Jing XL, Monson LA, Donneys A, Tchanque-Fossuo CN, Deshpande SS, Buchman SR. Deferoxamine reverses radiation induced hypovascularity during bone regeneration and repair in the murine mandible. Bone. 2012; 50(5): 1184-1187. doi:10.1016/j.bone.2012.01.019
24. Li Jia, Fan Lihong, Yu Zefeng, Dang Xiaoqian, Wang Kunzheng. The effect of deferoxamine on angiogenesis and bone repair in steroid-induced osteonecrosis of rabbit femoral heads. Exp. Biol. Med. (Maywood), 2015; 240(2): 273-80.doi:10.1177/1535370214553906.
25. Jia P, Chen H, Kang H, Qi J, Zhao P, Jiang M, Guo L, Zhou Q, Qian ND, Zhou HB, Xu YJ, Fan Y, Deng LF. Deferoxamine released from poly(lactic-co-glycolic acid) promotes healing of osteoporotic bone defect via enhanced angiogenesis and osteogenesis. J Biomed Mater Res A, 2016;104(10): 2515-27. doi:10.1002/jbm.a.35793.
26. Kusumbe Anjali P,Ramasamy Saravana K,Adams Ralf H,Coupling of angiogenesis and osteogenesis by a specific vessel subtype in bone. Nature. 2014; 507(7492): 323-328.doi: 10.1038/nature13145.
27. Park SB, Lee YJ and Chung CK. Bone mineral density changes after ovariectomy in rats as an osteopenic model: stepwise description of double dorso-lateral approach. J Korean Neurosurg Soc. 2010; 48(4): 309–312.doi:10.3340/jkns.2010.48.4.309.
28. Lelovas PP, Xanthos TT, Thoma SE, Lyritis GP, Dontas IA. The laboratory rat as an animal model for osteoporosis research. Comp Med. 2008; 58(5): 424–430.
29. Lucke M, Schmidmaier G, Sadoni S, Wildemann B, Schiller R, Stemberger A, Haas NP, Raschke M. A new model of implant-related osteomyelitis in rats. J. Biomed. Mater. Res. B. Appl. Biomater. 2003;67(1):593-602. doi:10.1002/jbm.b.10051.
30. Longhofer LK, Chong A, Strong NM, Wooley PH, Yang SY. Specific material effects of wear-particle-induced inflammation and osteolysis at the bone-implant interface: A rat model. J Orthop Translat. 2017; 8: 5-11. doi:10.1016/j.jot.2016.06.026.
31. Buvanendran A, Kroin JS, Kari MR, Tuman KJ. A new knee surgery model in rats to evaluate functional measures of postoperative pain. Anesth. Analg. 2008; 107(1): 300-8. doi:10.1213/ane.0b013e3181732f21.

32. Stadlinger B, Korn P, Tödtmann N, Eckelt U, Range U, Bürki A, Ferguson SJ, Kramer I, Kautz A, Schnabelrauch M. Osseointegration of biochemically modified implants in an osteoporosis rodent model. Eur. Cdll Mater. 2013;25:326-340.
33. Morris JL, Letson HL, Grant A, Wilkinson M, Hazratwala K, McEwen P. Staphylococcus aureusExperimental model of peri-prosthetic infection of the knee caused by using biomaterials representative of modern TKA. Biol Open, 2019, 8(9), undefined. doi:10.1242/bio.045203.
34. Søe NH, Jensen NV, Nürnberg BM, Jensen AL, Koch J, Poulsen SS, Pier G, Johansen HK. A novel knee prosthesis model of implant-related osteomyelitis in rats. Acta Orthop. 2013; 84(1): 92-7. doi: 10.3109/17453674.2013.773121.
35. Mann KA, Miller MA, Amendola RL, Cyndari KI, Horton JA, Damron TA, Oest ME. Early Changes in Cement-Bone Fixation Using a Novel Rat Knee Replacement Model. J. Orthop. Res. 2019; 37(10): 2163-2171. doi:10.1002/jor.24390.
36. Carli A. V, Bhimani S, Yang X, de Mesy Bentley KL, Ross FP, Bostrom MPG. Vancomycin-loaded polymethylmethacrylate spacers fail to eradicate periprosthetic joint infection in a clinically representative mouse model. J. Bone Joint Surg. 2018;100(11): e76.
37. Palmquist A, Omar OM, Esposito M, Lausmaa J, Thomsen P. Titanium oral implants: surface characteristics, interface biology and clinical outcome. J R Soc Interface. 2010; 6(Suppl. 5): 515–527. doi:10.1098/rsif.2010.0118.focus.
38. Pearce AI, Richards RG, Milz S, Schneider E, Pearce SG. Animal models for implant biomaterial research in bone: a review. Eur Cell Mater. 2007; 13:1–10. doi:10.22203/ecm.v013a01.
39. Wang GL, Jiang BH, Rue EA, Semenza GL. Hypoxia-inducible factor 1 is a basic-helix-loop-helix-PAS heterodimer regulated by cellular O2 tension. Proc Natl Acad Sci USA. 1995; 92(12):5510–5514. doi:10.1073/pnas.92.12.5510.
40. Riddle RC, Khatri R, Schipani E, Clemens TL. Role of hypoxia-inducible factor1alpha in angiogenic-osteogenic coupling. J Mol Med. 2009; 87: 583-90.
41. Wan C, Shao J, Gilbert SR, Riddle RC, Long F, Johnson RS. Role of HIF1alpha in skeletal development. Ann N Y Acad Sci. 2010; 1192: 322-6.
42. Genetos DC, Toupadakis CA, Raheja LF, Wong A, Papanicolaou SE, Fyhrie DP, Loots GG, Yellowley CE. Hypoxia decreases sclerostin expression and increases Wnt signaling in osteoblasts. J Cell Biochem. 2010;110(2):457–67. doi:10.1002/jcb.22559.
43. Kellesarian Sergio Varela, Abduljabbar Tariq, Vohra Fahim, Gholamiazizi Elham, Malmstrom Hans, Romanos Georgios E, Javed Fawad. Does Local Ibandronate and/or Pamidronate Delivery Enhance Osseointegration? A Systematic Review. J Prosthodont. 2018; 27(3), 240-249. doi:10.1111/jopr.12571
44. Farberg AS, Sarhaddi D, Donneys A, Deshpande SS, Buchman SR. Deferoxamine enhances bone regeneration in mandibular distraction osteogenesis. Plast. Reconstr. Surg. 2014; 133(3): 666-71. doi:10.1097/01.prs.0000438050.36881.a9.

45. Stewart R, Goldstein J, Eberhardt A, Chu GT, Gilbert S. Increasing vascularity to improve healing of a segmental defect of the rat femur. J Orthop Trauma. 2011; 25(8): 472-6. doi: 10.1097/BOT.0b013e31822588d8.
46. 46.Kang H, Yan Y, Jia P, Yang K, Guo C, Chen H, Qi J, Qian N, Xu X, Wang F, Li C, Guo L, Deng L. Desferrioxamine reduces ultrahigh-molecular-weight polyethylene-induced osteolysis by restraining inflammatory osteoclastogenesis via heme oxygenase-1. Cell Death Dis. 2016; 7(10): e2435. doi:10.1038/cddis.2016.339.
47. Drager J, Sheikh Z, Zhang YL, Harvey EJ, Barralet JE. Local delivery of iron chelators reduces in vivo remodeling of a calcium phosphate bone graft substitute. Acta Biomater. 2016; 42: 411-419. doi:10.1016/j.actbio.2016.07.037.
48. Yu Y, Ran Q, Shen X, Zheng H, Cai K. Enzyme responsive titanium substrates with antibacterial property and osteo/angio-genic differentiation potentials. Colloids Surf B Biointerfaces. 2020; 185(undefined):110592. doi:10.1016/j.colsurfb.2019.110592.
49. Melotte V, Qu X, Ongenaert M, van Criekinge W, de Bruïne AP, Baldwin HS, van Engeland M. The N-myc downstream regulated gene (NDRG) family: diverse functions, multiple applications. FASEB J. 2010;24(11):4153–66. doi:10.1096/fj.09-151464.
50. Xing W, Pourteymoor S, Mohan S. Ascorbic acid regulates osterix expression in osteoblasts by activation of prolyl hydroxylase and ubiquitination-mediated proteosomal degradation pathway. Physiol. Genomics. 2011;43(12):749-57. doi:10.1152/physiolgenomics.00229.2010 .
51. Li Wuyin, Cai Litao, Zhang Yun, Cui Lei, Shen Gan. Intra-articular resveratrol injection prevents osteoarthritis progression in a mouse model by activating SIRT1 and thereby silencing HIF-2a. J Orthop Res. 2015; 33(7): 1061-70. doi:10.1002/jor.22859.192

Figures

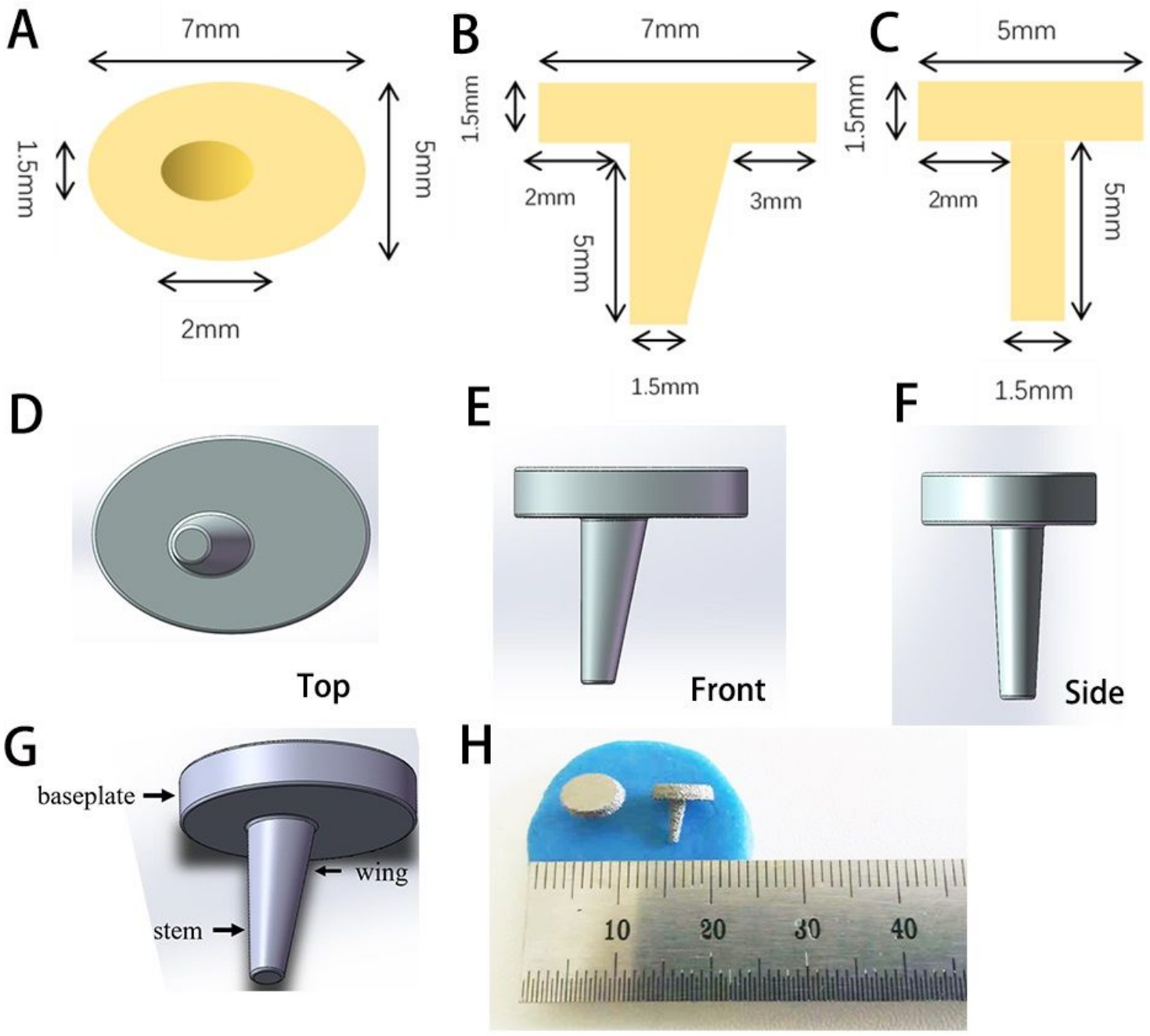

Figure 1

Measurement of rat tibial prosthesis in transverse, coronal and sagittal sections, 3D composite image and entity image.

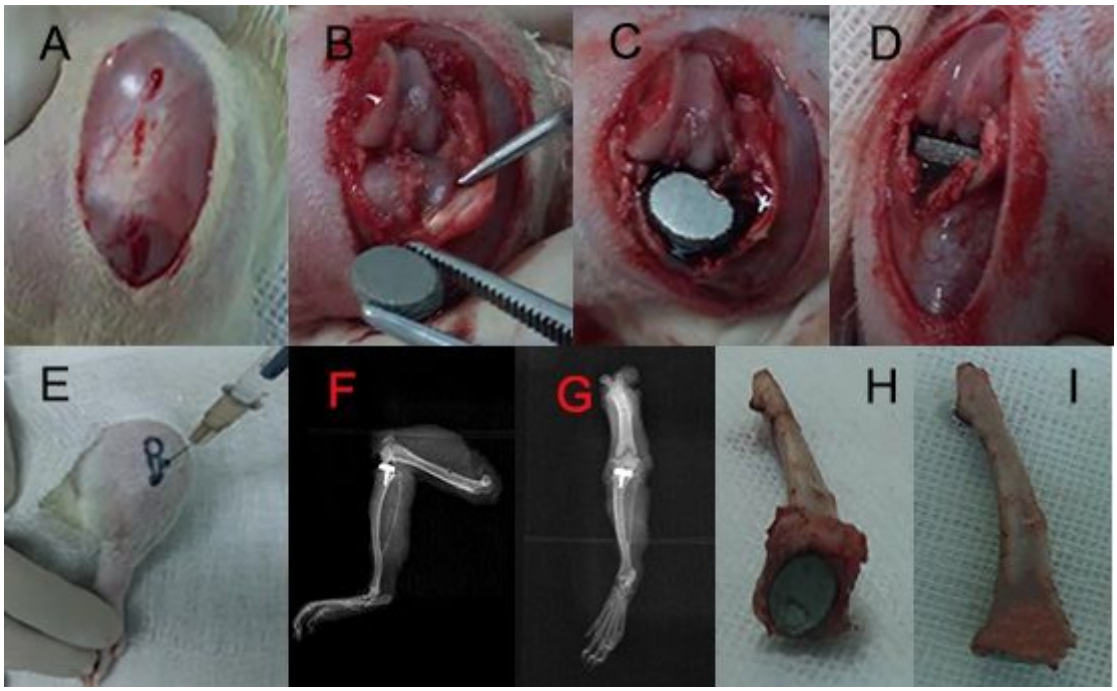

Figure 2

(A-D) The tibial plateau cartilage was replaced by 3D printed Prosthesis through hemiarthroplasty of knee. (E) Intraarticular injection of DFO through the medial approach beside patellar ligament. (F-G) Postoperative X-ray examination showed the position of implant is good. (H-I) Gross tibial specimen with prosthesis.

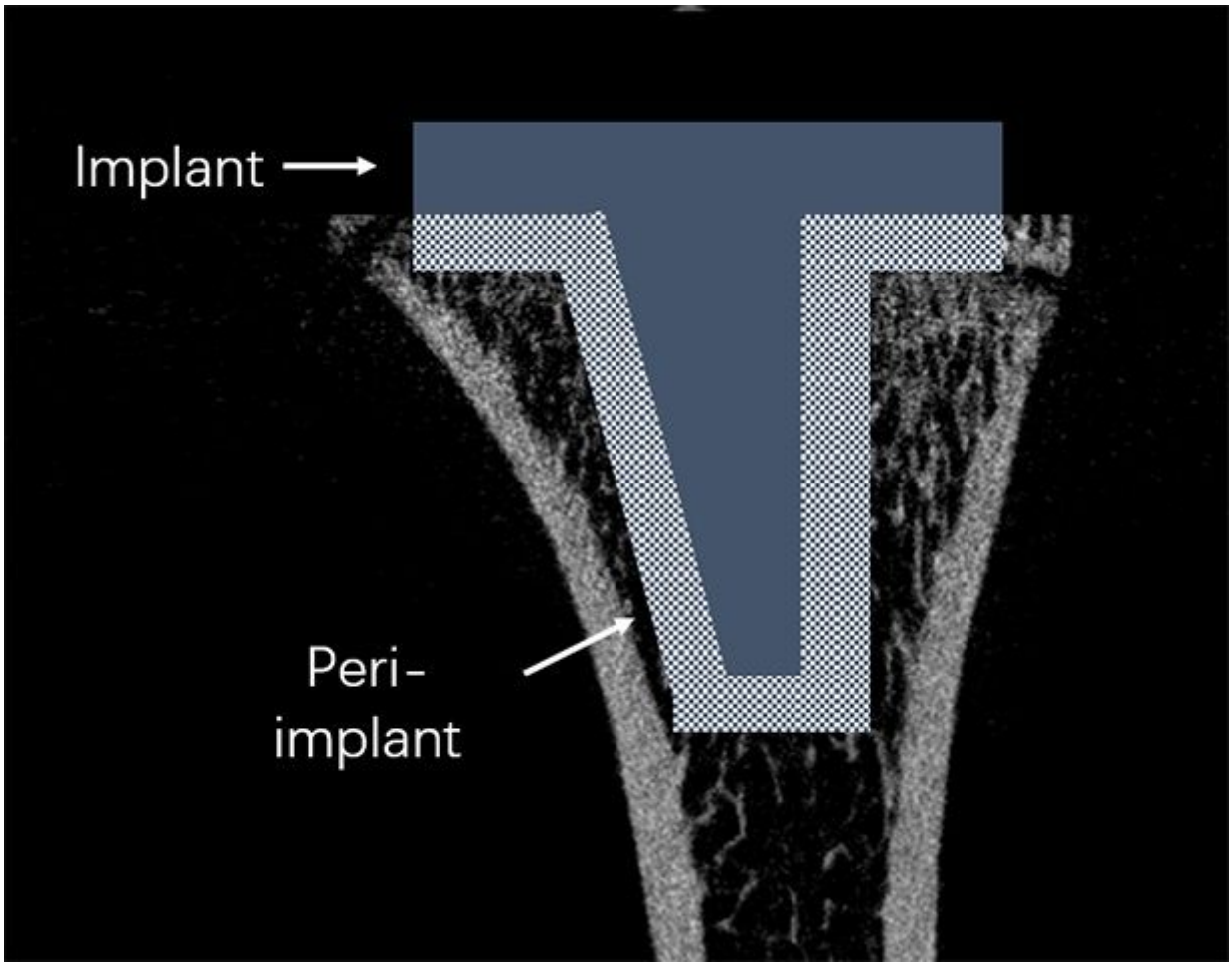

Figure 3

Volumes of interest for microCT measurements. 3 momths after operation, peri-implant bone adjacent to the distal 2mm of the implant was analyzed.

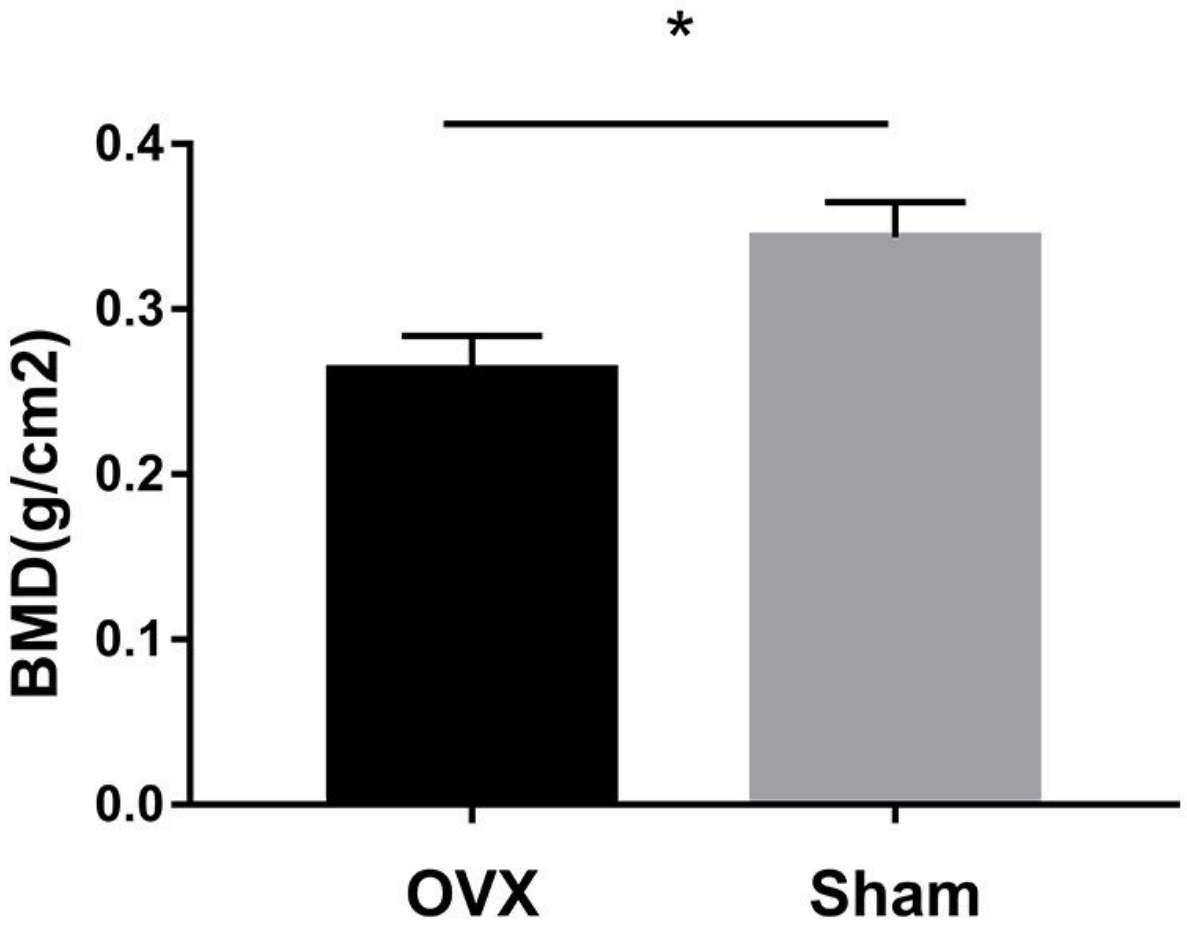

Figure 4

The BMD of trabecular bone in the OVX group was significantly lower than that of the sham group

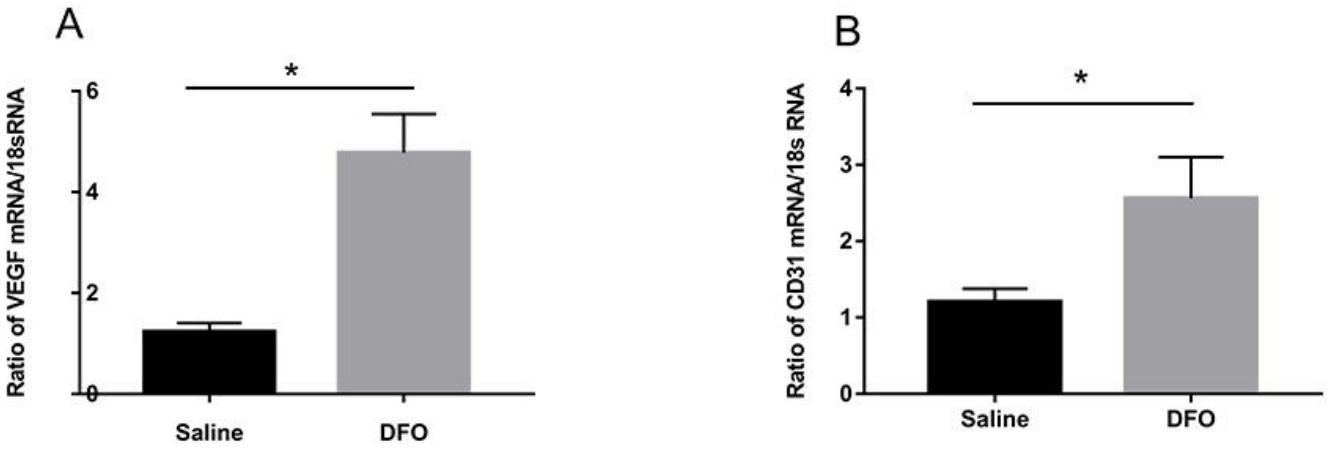

Figure 5

DFO activated the HIF-1a signaling pathway under normoxic conditions, which could significantly increas the mRNA expression levels of VEGF, thereby further improving the mRNA expression levels of CD31. (A) The mRNA expression levels of VEGF in both groups. (B) The mRNA expression levels of CD31 in both groups. An asterisk (*) indicates p<0.05.

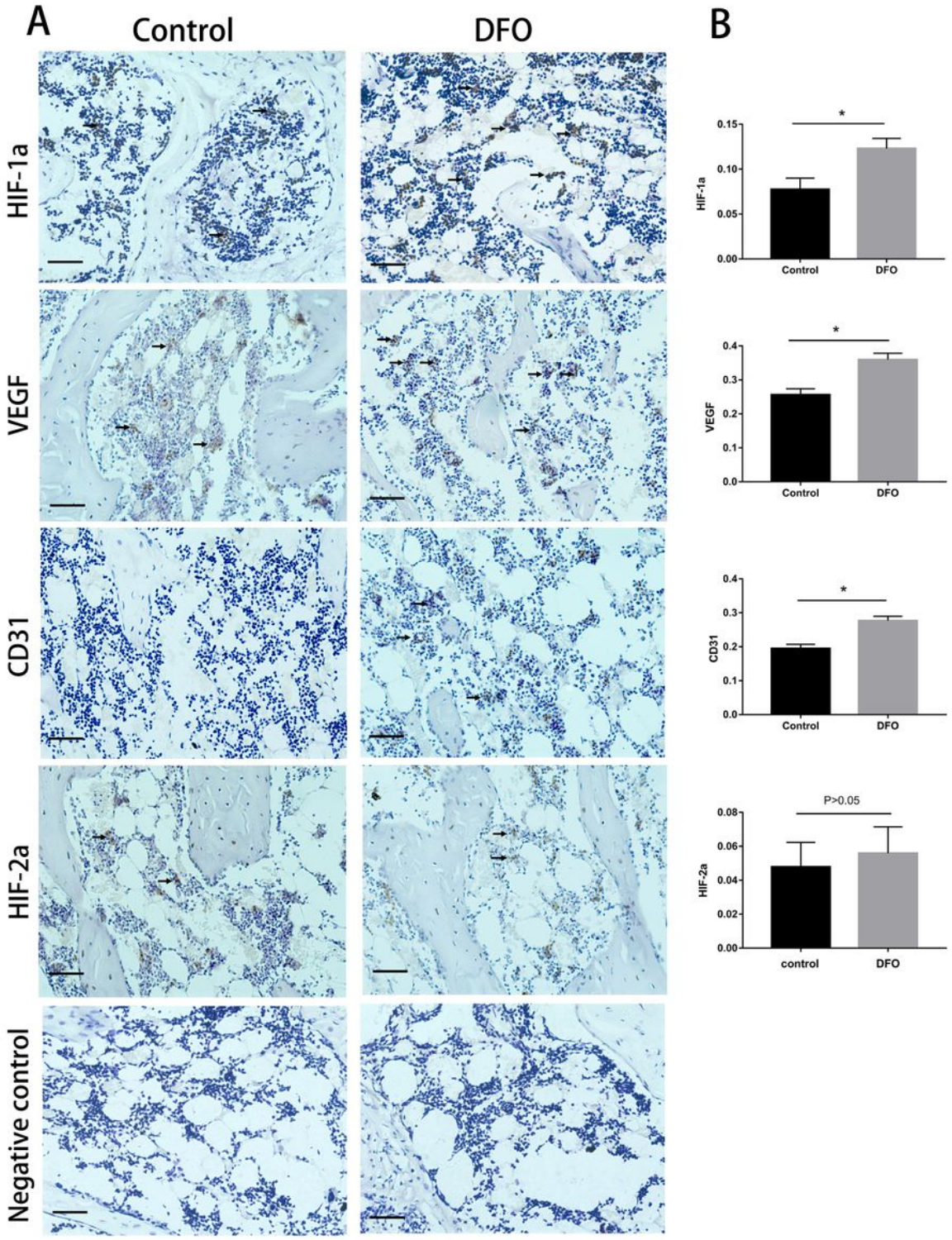

Figure 6

(A) Sections of new bone tissue around the implants were examined by Immunohistochemistry 2 weeks after surgery. Representative photomicrograph showed there were more HIF-1a, VEGF, and CD31 positive cells in the DFO group than in the control group. The CD31 was expressed clearly in clusters which indicated that there was more neovascularization. Only a small amount of HIF-2a was expressed in both groups. The appearance of brown substance indicated the antigen-positive staining and the black arrows point to them. (original magnification:200×per image, scale bars represent 50 μm). (B) Bar graphs showed the mean optical density of HIF-1a, VEGF and CD31 in bone tissue. Semiquantitative analysis was performed for eight sections (10 fields per section) in each group, and the difference was obvious. There was no difference for HIF-2a between the two groups. An asterisk (*) indicates $p<0.05$.

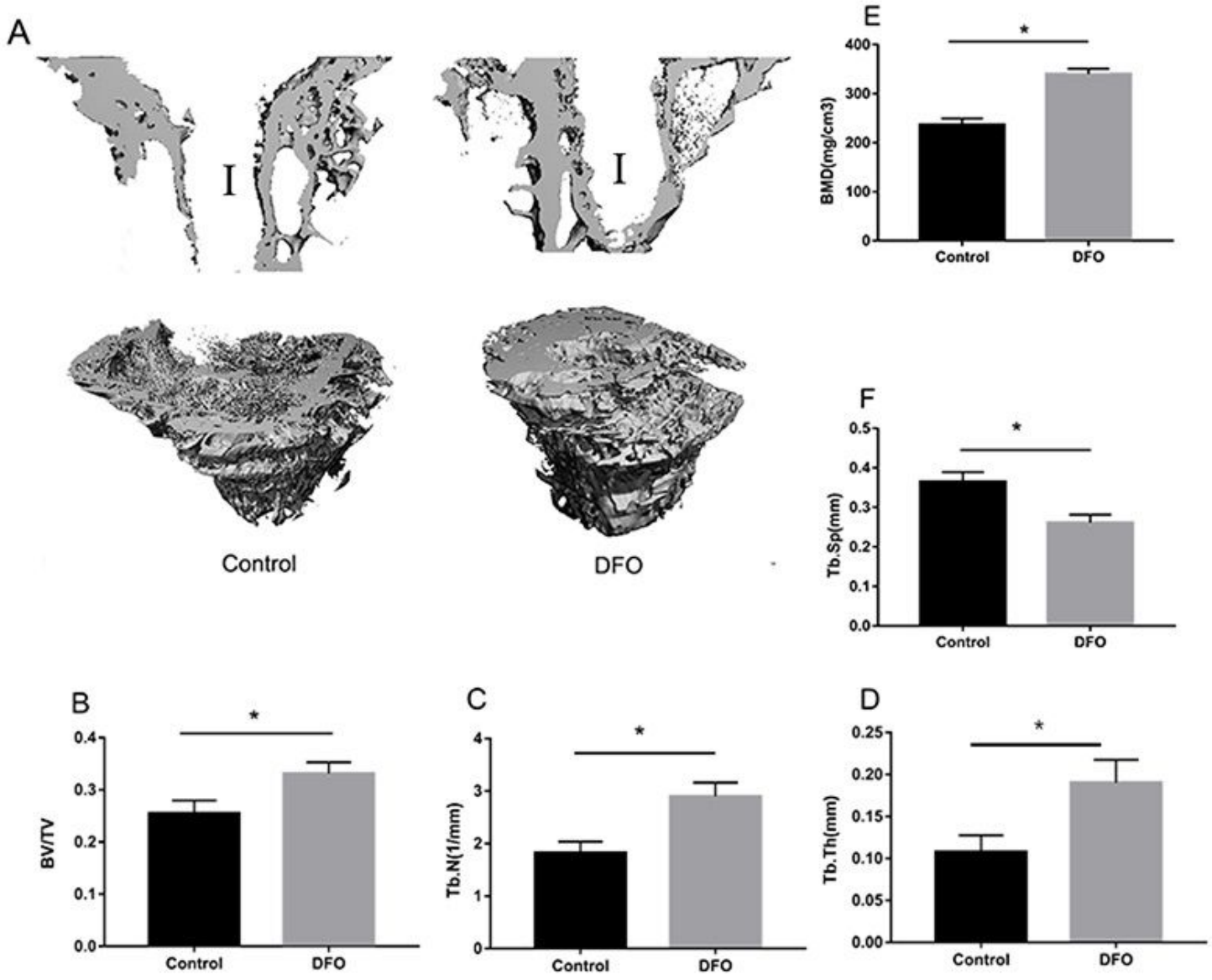

Figure 7

The bone formation around the prosthesis evaluated by micro-CT analysis. (A-F) 12 weeks after implanting surgery, = empty space after the implant was withdrawn, BV/TV, Tb.N, Tb.Th and BMD in the

DFO group over a uniform volume of interest were significantly higher than their measures in the control group, while Tb.Sp in DFO was much lower than that of control group. An asterisk (*) indicates p<0.05.

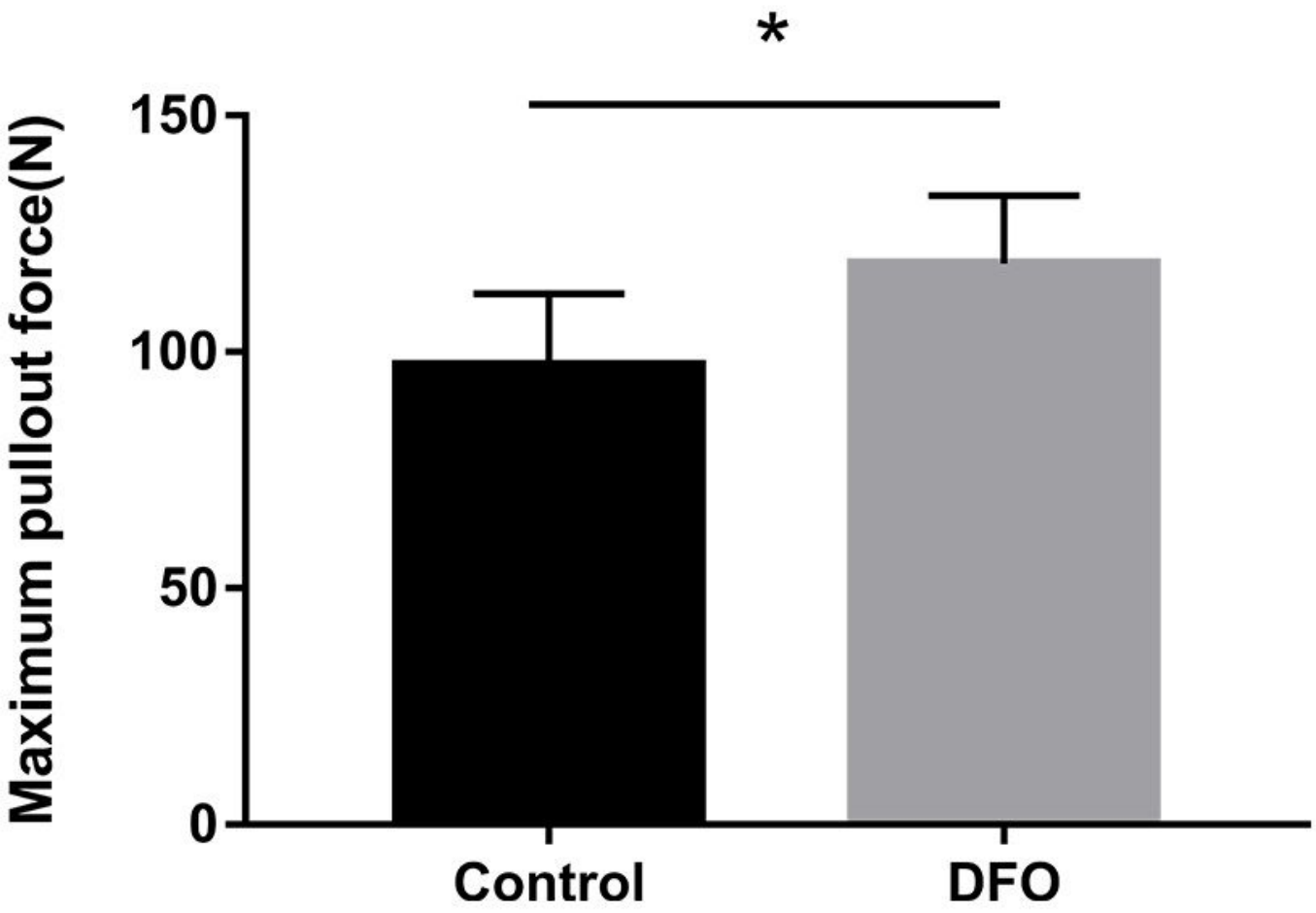

Figure 8

Biomechanics test result showed the maximum pullout force for DFO group was significantly higher than it was for control group. An asterisk (*) indicates p<0.05.

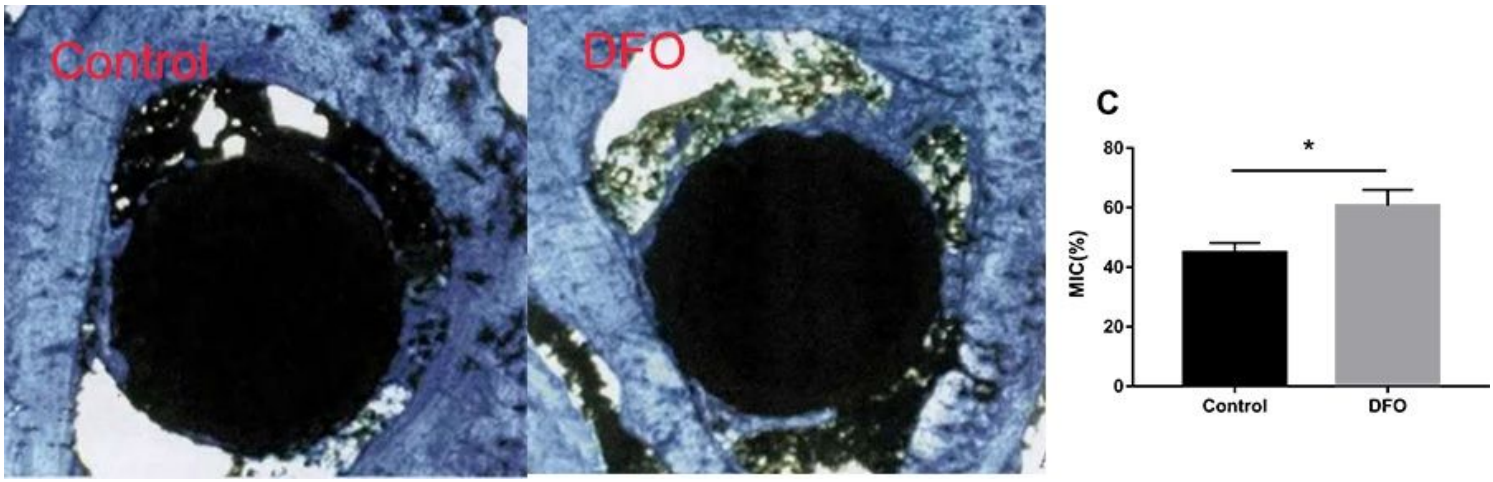

Figure 9

Histopathology result showed Bone-to-implant contact (BIC) value in DFO group was significantly higher than that in control group. An asterisk (*) indicates $p<0.05$.